

Oxygen-ion and electron conductivity in $\text{Sr}_2(\text{Fe}_{1-x}\text{Ga}_x)_2\text{O}_5$

I.A. Leonidov^a, M.V. Patrakeev^a, J.A. Bahteeva^a, K.V. Poholok^b, D.S. Filimonov^b,
K.R. Poeppelmeier^c, V.L. Kozhevnikov^{a,*}

^a*Institute of Solid State Chemistry, Ural Branch of RAS, Pervomaiskaia 91, Ekaterinburg 620219, Russia*

^b*Moscow State University, Vorob'evy gory, Moscow 119987, Russia*

^c*Department of Chemistry, Northwestern University, 2145 Sheridan Road, Evanston, IL 60208, USA*

Received 11 January 2006; received in revised form 24 April 2006; accepted 30 May 2006

Available online 3 June 2006

Abstract

High-temperature electrical conductivity measurements, structural data from powder X-ray diffraction and ^{57}Fe Mössbauer spectroscopy were combined to study the interrelationship of oxygen ion transport and p- and n-type transport in $\text{Sr}_2(\text{Fe}_{1-x}\text{Ga}_x)_2\text{O}_5$, where $x = 0, 0.1$ and 0.2 . Although gallium substitution generally decreases the total ion-electron transport, the transition of the orthorhombic brownmillerite structure to a cubic phase on heating results in the recurrence of the conductivity to the same high level as in the parent ferrite ($x = 0$). The changes of the partial contributions to the total conductivity as a function of x are shown to reflect a complicated interplay of the disordering processes that develop in the oxygen sublattice on heating in response to replacement of iron with gallium.

© 2006 Elsevier Inc. All rights reserved.

Keywords: Strontium ferrite; Mössbauer spectroscopy; Electrical conductivity

1. Introduction

The strontium ferrite, $\text{SrFeO}_{3-\gamma}$ is known as a typical mixed oxygen ion and electron conductor at elevated temperatures [1]. Decreasing the partial pressure of oxygen gives rise to an increase in the non-stoichiometry parameter such that in a reducing environment $\gamma = 0.5$ can be achieved [2,3]. At temperatures below 850°C the reduced ferrite $\text{SrFeO}_{2.5}$ crystallizes with the orthorhombic brownmillerite (OB) structure $\text{Sr}_2\text{Fe}_2\text{O}_5$ where vacancy ordering results in an alternation of layers of octahedra $\text{FeO}_{6/2}$ (O) and tetrahedra $\text{FeO}_{4/2}$ (T) along the b -axis [4–7]. Raising the temperature above 850°C results in transformation of the brownmillerite to a cubic structure that has long been thought of as a non-stoichiometric perovskite-like $\text{SrFeO}_{2.5}$ (cubic perovskite (CP)) [1,8,9]. It was shown, however, by in situ high-temperature neutron diffraction studies [10] that this cubic modification of $\text{Sr}_2\text{Fe}_2\text{O}_5$ (henceforth, cubic brownmillerite or CB) is characterized by the elementary

unit parameter $a \cong 2a_p$ of about twice larger than $a_p \cong 3.9 \text{ \AA}$ in the non-stoichiometric perovskite-like $\text{SrFeO}_{2.5}$ (CP) which becomes stable on heating at about $950\text{--}1000^\circ\text{C}$. It is interesting to observe that the oxygen ion conductivity in both OB and CB structures, though smaller than in the CP phase, is nonetheless quite appreciable. Because vacancy ordering in the OB and CB structures is far from ideal, incipient disordering of oxygen vacancies and oxygen ions manifests itself in noticeable changes of conductivity in the ferrite at relatively low temperatures near 600°C [11].

Partial replacement of iron in $\text{Sr}_2\text{Fe}_2\text{O}_5$ for gallium, where gallium is known to have a strong preference for tetrahedral coordination by oxygen, can have a considerable influence on the disordering of the oxygen vacancies and the oxygen ions, the OB \rightarrow CB phase transition temperature, and, eventually, the oxygen ion and electron transport. In this work, we studied the electrical conductivity of the gallium-substituted oxides $\text{Sr}_2(\text{Fe}_{1-x}\text{Ga}_x)_2\text{O}_5$ at different temperatures and partial pressures of oxygen. Additionally, Mössbauer spectroscopy was utilized in order to study the local environment of the iron ions. The contributions to the total conductivity from the

*Corresponding author. Fax: +7 3432 74 00 03.

E-mail address: kozhevnikov@imp.uran.ru (V.L. Kozhevnikov).

oxygen ions, electrons and electron holes were derived based on their dependence on the oxygen partial pressure. The variations of these partial contributions with temperature and gallium content are discussed.

2. Experimental

The specimens $\text{SrFe}_{1-x}\text{Ga}_x\text{O}_{3-\gamma}$, where $x = 0, 0.1$ and 0.2 , were synthesized by heating in air at $900\text{--}1250\text{ }^\circ\text{C}$ either appropriate mixtures of high grade purity oxides Fe_2O_3 , Ga_2O_3 and strontium carbonate SrCO_3 , or mixtures of dehydrated co-precipitates $\text{Fe}(\text{OH})_3/\text{Ga}(\text{OH})_3$ with strontium oxide. The hydroxide precursors were obtained by addition of ammonium hydroxide to water solutions of iron and gallium nitrates. The co-precipitates were dried in air at $250\text{ }^\circ\text{C}$ and then mixed with appropriate amount of freshly prepared strontium oxide in a dry box. The strontium oxide was obtained immediately before use by thermolysis under dynamic vacuum of strontium carbonate at $950\text{ }^\circ\text{C}$. The synthesized powders were ball milled and pressed under 1 kbar of uniaxial load in pellets with the thickness of about 2 mm and the diameter of 20 mm. The pellets were sintered for 10 h in the air at $1250\text{ }^\circ\text{C}$ and cooled down to room temperature with the rate of $2^\circ/\text{min}$. The density of the ceramic samples was about 90% of theoretical. The specimens with reduced oxygen content corresponding to the formula $\text{Sr}_2(\text{Fe}_{1-x}\text{Ga}_x)_2\text{O}_5$ were obtained by firing the air synthesized materials in the flow of commercial He at $900\text{ }^\circ\text{C}$, or in the gas mixture He (5% H_2) at $700\text{ }^\circ\text{C}$. Phase purity control and determination of the crystal lattice parameters were carried out with X-ray diffraction using a STADI-P (STOE) diffractometer in Bragg–Brentano geometry ($\text{CuK}\alpha$ radiation, 2θ range of $5\text{--}120^\circ$, step 0.02° , acquisition time 4 s).

Rectangular bars $2 \times 2 \times 18\text{ mm}$ were cut from the sintered pellets for d.c. conductivity (σ) measurements. Current leads of platinum wire (0.3 mm) were tightly wound to the sample at 14 mm spacing while the spacing between the potential probes was 8 mm. The measurements were carried out in a cell utilizing oxygen sensing and pumping properties of cubic zirconia as described elsewhere [12]. The cell was filled with a 50% O_2 , 50% CO_2 gas mixture in the beginning of the experiment and sealed. The electrical parameters were measured with a high-precision SOLARTRON 7081 voltmeter. The measurements were carried out in isothermal runs. The equilibration time after a change of the oxygen pressure inside the cell varied from several dozen minutes to several hours depending on temperature and oxygen pressure in the cell. The measurements were halted upon achievement of the desirable low-pressure limit. Then the oxygen pressure was increased to the starting upper limit and the measurements repeated to confirm reversibility of the experiment; thereupon temperature was changed thus enabling the next measuring cycle. The errors in the experimental conductivity data were related mainly to measurements of geometrical sizes and did not exceed 10%.

Mössbauer spectra were obtained with an electrodynamic spectrometer in the mode of permanent acceleration. The data were computer processed with standard software for minimization of square functionals. The ^{57}Co isotope with activity of 0.45 GBq was imbedded in the rhodium metal matrix and used as a gamma-rays source. The obtained chemical shifts were referred to $\alpha\text{-Fe}$ at room temperature.

3. Results and discussion

3.1. Structural features

The X-ray powder diffraction patterns give evidence of a brownmillerite-like structure in the samples $\text{Sr}_2(\text{Fe}_{1-x}\text{Ga}_x)_2\text{O}_5$ with $x = 0, 0.1$ and 0.2 ($a \approx \sqrt{2}a_p$, $b \approx 4a_p$, $c \approx \sqrt{2}a_p$, where $a_p \approx 3.9$ [7]) (see Table 1). Attempts to incorporate larger amount of gallium, $x = 0.3$, resulted in appearance of additional phases. It can be seen from Table 1 that the elementary cell parameters are appreciably smaller in the sample $x = 0.1$ than in $x = 0$. This change can be explained assuming that the smaller Ga^{3+} cations replace Fe^{3+} cations [13] in the T-layers, which is consistent with the strong preference of gallium for tetrahedral coordination. The Mössbauer study was undertaken in order to gain more insight into distribution of gallium cations.

The Mössbauer spectra of ^{57}Fe in $\text{Sr}_2(\text{Fe}_{1-x}\text{Ga}_x)_2\text{O}_5$ at 100 K are shown in Fig. 1. The spectra can be described as a superposition of two Zeeman sextets (Table 2). The sextet with larger values of the isomer chemical shift ($\delta \approx 0.50\text{ mm/s}$) and of the hyperfine magnetic field ($H \approx 540\text{ kOe}$) corresponds to iron cations Fe_O^{3+} in distorted octahedral oxygen coordination, while the sextet with smaller values ($\delta \approx 0.35\text{ mm/s}$, $H \approx 453\text{ kOe}$) is due to iron cations Fe_T^{3+} in a distorted tetrahedral oxygen environment. The strong distortions of the oxygen polyhedra follow from large quadrupole shifts of the spectral lines, which are close to those in $\text{Sr}_2\text{Fe}_2\text{O}_5$ ($\varepsilon = -0.28\text{ mm/s}$ for Fe_O^{3+} and $\varepsilon = 0.30\text{ mm/s}$ for Fe_T^{3+}). It should be noticed that the chemical shifts for Fe_O^{3+} and Fe_T^{3+} do not significantly change with gallium content, which demonstrates the iron–oxygen chemical bonds do not change in any significant way at the doping levels used in this work. Comparison of the experimental spectra in Fig. 1 shows that partial replacement of Fe^{3+} for diamagnetic Ga^{3+} cations results mainly in decrease of the spectral component corresponding to Fe_T^{3+} . Considering the small difference of the Lamb–Mössbauer factors for Fe_O^{3+} and

Table 1
The elementary unit parameters in the samples of $\text{Sr}_{1-x}\text{Ga}_x\text{O}_{3-\gamma}$ obtained after heat treatment at $700\text{ }^\circ\text{C}$ in 5% $\text{H}_2/95\%$ He gas mixture

x	a (Å)	b (Å)	c (Å)
0.0	5.668(5)	15.582(3)	5.526(5)
0.1	5.647(9)	15.561(1)	5.510(4)
0.2	5.646(1)	15.553(6)	5.505(7)

Fe_T^{3+} in $\text{Sr}_2\text{Fe}_2\text{O}_5$ [14], the assertion can be made that Ga^{3+} cations in $\text{Sr}_2(\text{Fe}_{1-x}\text{Ga}_x)_2\text{O}_5$ replace predominantly iron in the layers of tetrahedra, which is consistent with the analysis of the concentration-dependent behavior of the lattice parameters. At the same time, a more precise evaluation on the basis of the spectral areas $A(\text{Fe}_O^{3+})$ and $A(\text{Fe}_T^{3+})$ for O- and T-sites, respectively, gives additional evidence that a small (and increasing with doping) amount of gallium substitutes for iron in the layers of octahedra (see Table 2). It should be noticed also from parameter Γ in Table 2 that gallium substitution results in considerable broadening of the Zeeman sextets. This broadening reflects the fact that the second coordination spheres of Fe_O^{3+} and Fe_T^{3+} include different cation configurations. Generally, the experimental data suggest that the structural disordering, which occurs in response to gallium incorporation in $\text{Sr}_2(\text{Fe}_{1-x}\text{Ga}_x)_2\text{O}_5$, can be represented by the crystallochemical formula

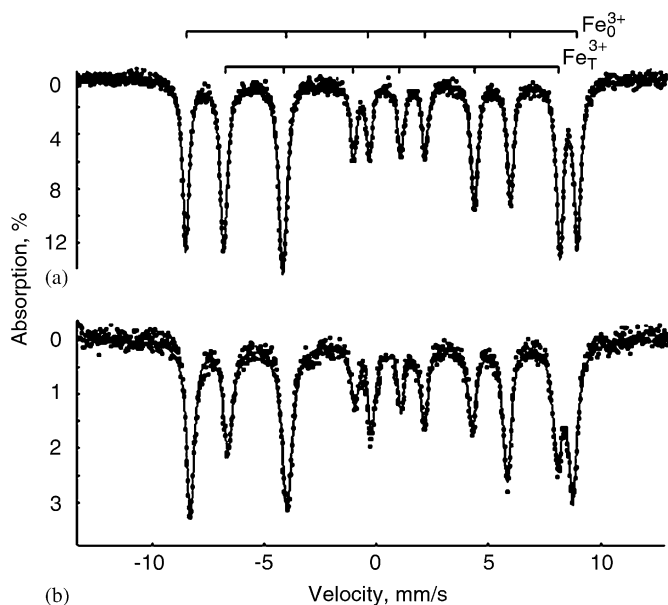
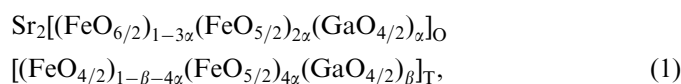
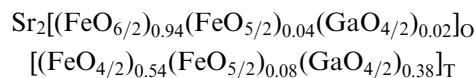


Fig. 1. The ^{57}Fe Mössbauer spectra for $\text{Sr}_2(\text{Fe}_{1-x}\text{Ga}_x)_2\text{O}_5$ at 80 K: = 0 (a) and = 0.2 (b).

Table 2
The Mössbauer spectra parameters for ^{57}Fe in $\text{Sr}_2(\text{Fe}_{1-x}\text{Ga}_x)_2\text{O}_5$ at 80 K

Compound		δ (mm/s) ± 0.02	ε (mm/s) ± 0.02	H (kOe) ± 3	Γ (mm/s) ± 0.02	A (%) ± 2
$\text{SrFeO}_{2.5}$	Fe_O^{3+}	0.52	-0.28	542	0.32	50
	Fe_T^{3+}	0.31	0.30	455	0.33	50
$\text{SrFe}_{0.90}\text{Ga}_{0.10}\text{O}_{2.5}$	Fe_O^{3+}	0.55	-0.29	536	0.42	54
	Fe_T^{3+}	0.32	0.29	450	0.43	46
$\text{SrFe}_{0.80}\text{Ga}_{0.20}\text{O}_{2.5}$	Fe_O^{3+}	0.53	-0.28	540	0.45	61
	Fe_T^{3+}	0.31	0.31	451	0.45	39

where O- and T- layers are shown with square brackets, while parameters α and β are interrelated as $\alpha + \beta = 2x$, and α is substantially smaller than β . In particular, the spectral areas $A(\text{Fe}_O^{3+})$ and $A(\text{Fe}_T^{3+})$ in Table 2 enable one to represent the oxide $x = 0.2$ at the solubility border as



or, in shorter notation, as $\text{Sr}_2[\text{Fe}_{0.98}\text{Ga}_{0.02}]_{\text{O}}[\text{Fe}_{0.62}\text{Ga}_{0.38}]_{\text{T}}\text{O}_5$.

3.2. Oxygen-ion conductivity

The experimental isotherms of the total conductivity vs. oxygen partial pressure are shown in Fig. 2. The conductivity increase with the pressure to the right of the minima shows the presence of the electron hole contribution (σ_p), while a similar increase with the pressure decrease to the left of the minima signals the electron contribution (σ_n). Rather small, and decreasing with the temperature increase, changes in conductivity with variations of oxygen pressure are indicative of the appreciable oxygen-ion (σ_i) component. Therefore, the measured values for the conductivity near the minima were modeled with the known relation

$$\sigma = \sigma_i + \sigma_n^0 p\text{O}_2^{-1/4} + \sigma_p^0 p\text{O}_2^{+1/4}, \quad (2)$$

where σ_i is the pressure independent ion contribution and σ_n^0 and σ_p^0 represent electron and hole components, respectively, extrapolated to $p\text{O}_2 = 1$ atm. The parameters σ_i , σ_n^0 and σ_p^0 , which provide an excellent fit of the experimental data, are given in Table 3. The sum of electron and hole contributions ($\sigma_{n+p} = \sigma_n + \sigma_p$) can be obtained by subtracting the ion contribution from the total conductivity (see Fig. 3). The plots in Fig. 3 confirm that near the minima the electron and hole components change with the pressure as $\sigma_n \sim p\text{O}_2^{-1/4}$ and $\sigma_p \sim p\text{O}_2^{+1/4}$, respectively.

The oxygen-ion conductivity is shown with Arrhenius coordinates in Fig. 4. At temperatures below 800 °C, where the OB structure is stable in all the samples ($x = 0, 0.1$ and 0.2), the oxygen-ion conductivity is relatively small and strongly varies with the gallium content. The very large activation energy (~ 3 eV) can be interpreted as evidence of

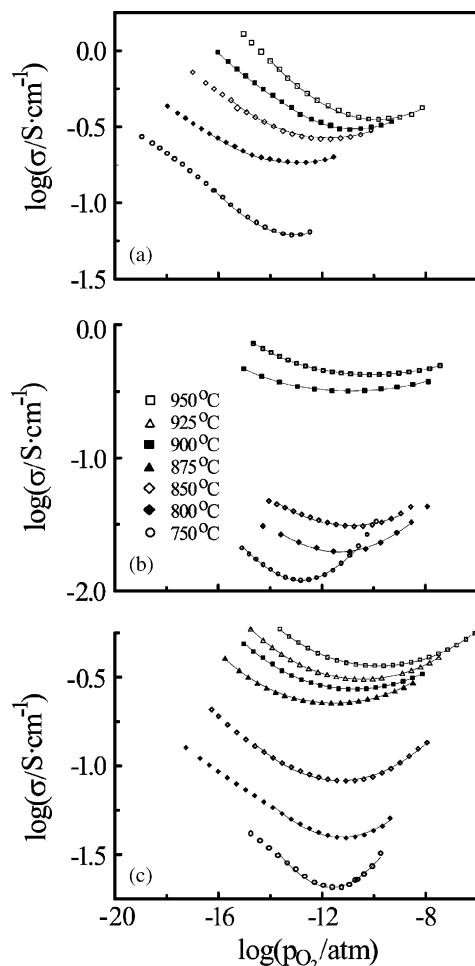


Fig. 2. The experimental results for changes in the total conductivity of $\text{Sr}_2(\text{Fe}_{1-x}\text{Ga}_x)_2\text{O}_5$ with oxygen partial pressure at different temperatures: $x = 0$ (a), 0.1 (b) and 0.2 (c). Solid lines show results of the fitting according to Eq. (2).

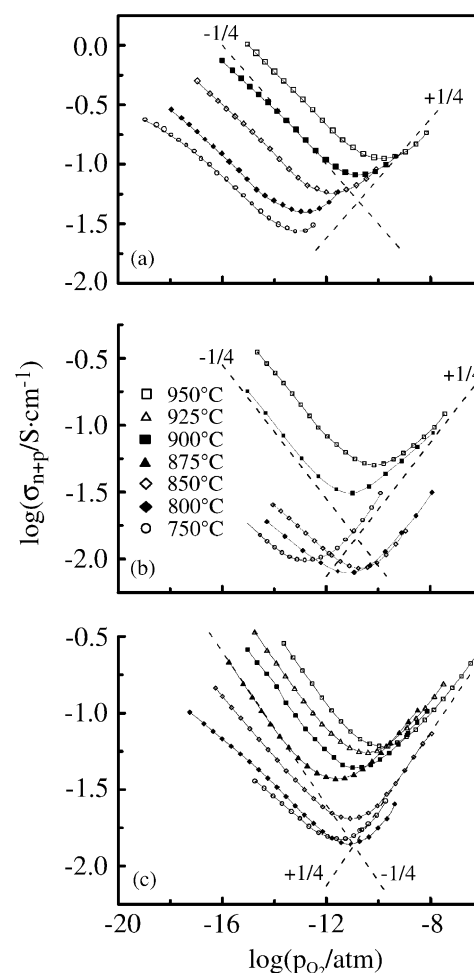


Fig. 3. The isothermal logarithmic plots for the sum of electron and hole contributions in $\text{Sr}_2(\text{Fe}_{1-x}\text{Ga}_x)_2\text{O}_5$ versus oxygen partial pressure: $x = 0$ (a), 0.1 (b) and 0.2 (c). Dashed lines show slopes proportional to $p\text{O}_2^{\pm 1/4}$.

Table 3
The conductivity parameters in Eq. (2) for $\text{Sr}_2(\text{Fe}_{1-x}\text{Ga}_x)_2\text{O}_5$

x	T (°C)	Parameter		
		σ_i (S cm^{-1})	σ_n^o (S cm^{-1})	σ_p^o (S cm^{-1})
0	950	0.24	1.9×10^{-4}	16.9
	900	0.22	8.9×10^{-5}	20.1
	850	0.21	3.5×10^{-5}	25.4
	800	0.14	1.2×10^{-5}	36.1
	750	0.04	6.7×10^{-6}	16.7
0.1	950	0.37	7.7×10^{-5}	8.4
	900	0.29	3.1×10^{-5}	8.4
	850	2.1×10^{-2}	8.5×10^{-6}	2.4
	800	1.1×10^{-2}	6.0×10^{-6}	2.7
	750	2.2×10^{-3}	3.0×10^{-6}	7.9
0.2	950	0.31	1.1×10^{-4}	8.5
	900	0.23	4.6×10^{-5}	10.7
	850	0.07	2.1×10^{-5}	5.5
	800	0.03	1.1×10^{-5}	4.7
	750	5.6×10^{-3}	9.0×10^{-6}	6.1

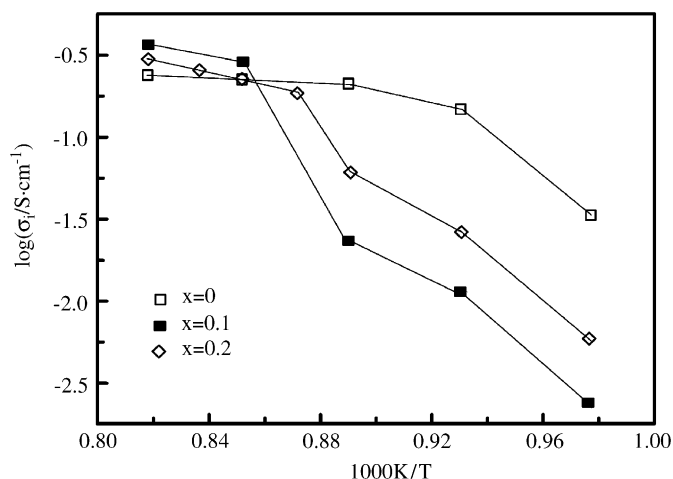


Fig. 4. Arrhenius plots for the ion conductivity in $\text{Sr}_2(\text{Fe}_{1-x}\text{Ga}_x)_2\text{O}_5$: $x = 0$ (\square), $x = 0.1$ (\blacksquare) and $x = 0.2$ (\diamond).

the temperature driven disordering of the OB framework that involves oxygen anions and vacancies in the layers of octahedra and tetrahedra, respectively [11]. Moreover, it

follows from the conductivity values that most intense disordering occurs in the parent ferrite $\text{Sr}_2\text{Fe}_2\text{O}_5$, while substitution of gallium in the layers of tetrahedra (as described before, see Section 3.1) results in a more rigid structure and the exclusion of a number of oxygen vacancies, possibly adjacent to gallium cations, from the oxygen-ion transport network. Thus, the oxygen-ion conductivity in the gallium-substituted derivatives is inferior compared to $\text{Sr}_2\text{Fe}_2\text{O}_5$. As discussed before, the Mössbauer spectroscopy data indicate that a small number of gallium tetrahedra are in the octahedral layers, especially between $x = 0.1$ and 0.2 . This can help to understand the changes in conductivity in the OB structure at $x = 0.1$ versus at $x = 0.2$. Indeed, according to the suggested structural disordering, and as it follows from the crystallo-chemical formula (1) for the OB phase, replacement of $\text{FeO}_{6/2}$ octahedra with $\text{GaO}_{4/2}$ tetrahedra is accompanied with the simultaneous formation of twice the number of square pyramids $\text{FeO}_{5/2}$ and additional oxygen vacancies in the octahedral layers. These “induced” vacancies apparently favor enhanced oxygen-ion conductivity when $x = 0.2$ compared to the composition $x = 0.1$.

Further heating results in an increase in the conductivity, such that at temperatures near 900°C the conductivity values approach about 0.2 S/cm and then cease to viably depend on the gallium content. Considering that the change in the temperature dependence of conductivity in $\text{Sr}_2\text{Fe}_2\text{O}_5$ reflects the OB \rightarrow CB transition [10], we surmise that preservation of the OB structure in the gallium-substituted derivatives on heating becomes unfavorable too, and on accumulation of a certain level of disorder the orthorhombic structure transforms to some other structural type. It is natural to suppose that this high-temperature modification of the gallium-substituted samples bears a close resemblance to the high-temperature CB structure of $\text{Sr}_2\text{Fe}_2\text{O}_5$. The proposal is supported by and is consistent with the observation that the conductivity is practically independent of the gallium substitution. Although the exact structure of the CB phase was not established in [10] it may be that essential structural features include five-fold, nearly pyramidal oxygen coordination of some percentage the iron/gallium cations and some ordering of oxygen vacancies. This model is consistent with the reduced conductivity of the CB phase compared to CP phase with completely or nearly random oxygen vacancies [1].

3.3. Electron *p*- and *n*-type conductivity

The hole conductivity at $p\text{O}_2 = 10^{-8}$ atm was calculated as $\sigma_p = \sigma_p^0 p\text{O}_2^{+1/4}$ with the values for σ_p^0 from Table 3. The temperature dependences obtained for different samples are shown with Arrhenius coordinates in Fig. 5. The positive slope of the plot $\log \sigma_p$ vs. T^{-1} for $\text{Sr}_2\text{Fe}_2\text{O}_5$ at high temperatures, i.e. in the CB phase, is indicative of the exothermal oxidation reaction:

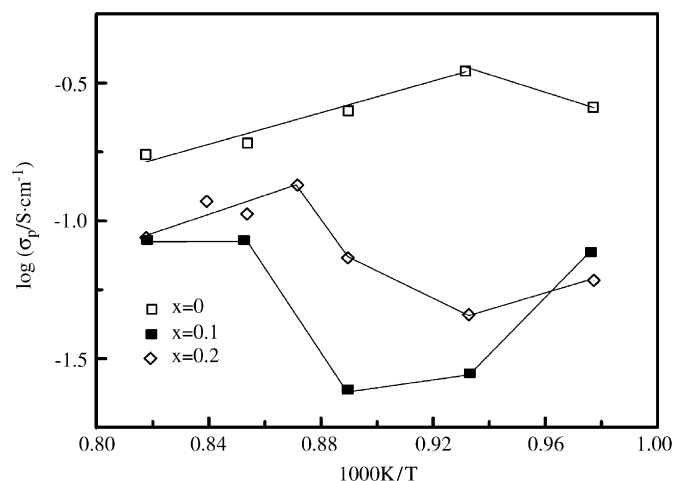
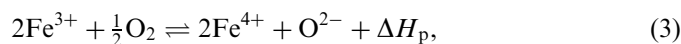


Fig. 5. Arrhenius plots for the hole conductivity in $\text{Sr}_2(\text{Fe}_{1-x}\text{Ga}_x)_2\text{O}_5$ at 10^{-8} atm: $x = 0$ (\square), $x = 0.1$ (\blacksquare) and $x = 0.2$ (\diamond).

where ΔH_p is the oxidation enthalpy. It follows from the reaction equation that the activation energy E_p for the hole conductivity is equal to $E_p = \varepsilon_p + \Delta H_p/2$, where ε_p is the hole mobility activation energy. Assuming the inequality $\varepsilon_p \ll \Delta H_p$, the reaction enthalpy can roughly be estimated as $\Delta H_p \approx 2E_p$. The experimental data in Fig. 5 result in $E_p = -0.45\text{ eV}$, which gives $\Delta H_p \approx -0.9\text{ eV}$. This value for ΔH_p is rather close to the partial molar enthalpy for oxygen incorporation ($\Delta H_O = -1.03\text{ eV}$) obtained from the $p\text{O}_2$ - T - γ diagram for the non-stoichiometric ferrite $\text{SrFeO}_{3-\gamma}$ at $\gamma \rightarrow 0.5$ [15]. Values for ΔH_p and ΔH_O should be equal [16] when compared at equal stoichiometry. Hence, the difference between ΔH_p and ΔH_O can be ascribed to the hole mobility activation energy of about 0.06 – 0.07 eV .

The changes in the slope of the isobars in Fig. 5 on cooling from high temperatures are likely interrelated with the CB \rightarrow OB transition and the formation of tetrahedral layers unfavorable for electron hole transport. Because vacancy ordering is more intensive in the samples that contain gallium, “switching off” of the tetrahedral layers from the hole transport manifests itself in a considerable conductivity decrease with temperature in the samples containing gallium compared to $\text{Sr}_2\text{Fe}_2\text{O}_5$. Further cooling of compounds with $x = 0.1$ and 0.2 reveals an unusual increase in the hole conductivity with temperature decreases below about 830°C . This too can be understood as reflecting intercalation of a small amount of the off-stoichiometric oxygen in the layers of tetrahedra, which in the gallium substituted samples does not exceed 1% of the total oxygen content at $p\text{O}_2 = 10^{-8}$ atm and $T < 850^\circ\text{C}$.

The n-type contribution to conductivity, calculated as $\sigma_n = \sigma_n^0 p\text{O}_2^{-1/4}$, at $p\text{O}_2 = 10^{-16}$ atm exhibits temperature activated character (Fig. 6). The structural phase transition CB \rightarrow OB on cooling results in the decrease of the conductivity activation energy from 1.9 eV in the cubic phase to about 1.0 eV in the OB phase. Because

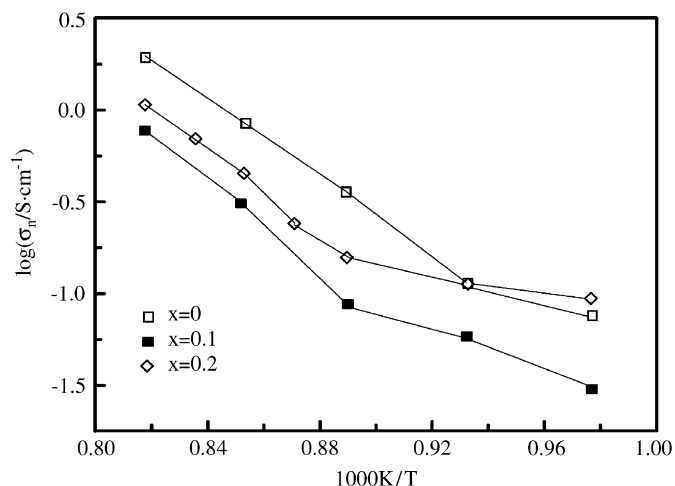
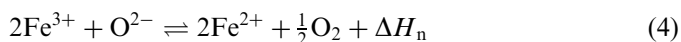


Fig. 6. Arrhenius plots for the electron conductivity in $\text{Sr}_2(\text{Fe}_{1-x}\text{Ga}_x)_2\text{O}_5$ at 10^{-16} atm: $x = 0$ (□), $x = 0.1$ (■) and $x = 0.2$ (◇).

non-intrinsic electrons (Fe^{2+} cations) appear in $\text{Sr}_2(\text{Fe}_{1-x}\text{Ga}_x)_2\text{O}_5$ in response to the reaction



where ΔH_n is the reaction enthalpy, the apparent activation energy for conductivity $E_n = \varepsilon_n + \Delta H_n/2$ includes energy contributions necessary for migration (ε_n) and formation ($\Delta H_n/2$) of electron carriers. It can be seen from the expression for E_n that one of the reasons for the large difference in the activation energy in the CB and OB phases can be related to the migration energy being larger in the CB phase than in the more ordered brownmillerite phase. However, more probable is that so large a difference reflects a larger reduction enthalpy [17]. This may in fact be the case because oxygen depletion in the cubic phase takes place from a pyramidal environment of Fe^{3+} cations, while in the OB oxygen anions are scavenged from iron–oxygen octahedra where the Coulomb binding energy per oxygen ion is smaller than in the pyramid at environment. It should be noticed that the partial components of the conductivity σ_n and σ_p are both smaller in the gallium-doped samples than in the parent ferrite $\text{Sr}_2\text{Fe}_2\text{O}_5$, reflecting a general decrease in the mobility of both types of carriers caused by the decrease in the amount of electro-active iron sites.

4. Conclusions

Electrical conductivity measurements carried out on $\text{Sr}_2(\text{Fe}_{1-x}\text{Ga}_x)_2\text{O}_5$, where $x = 0, 0.1$ and 0.2 , within the temperature range $750\text{--}950^\circ\text{C}$ and at oxygen partial pressures between 10^{-19} and 10^{-6} atm were used to determine variations of the total conductivity with oxygen pressure in order to determine partial contributions from oxygen ions, electron holes and electrons. An analysis of the influence of the temperature and gallium substitution upon transport properties, carried out taking into regard X-ray diffraction and ^{57}Fe Mössbauer spectroscopy data,

demonstrated that replacement of iron with gallium in the brownmillerite structure of $\text{Sr}_2(\text{Fe}_{1-x}\text{Ga}_x)_2\text{O}_5$ with $x = 0.1$ occurs as incorporation of $\text{GaO}_{4/2}$ tetrahedra in the $\text{FeO}_{4/2}$ structural layers. The gallium cations in these tetrahedral layers favor exclusion of the neighboring oxygen vacancies from the transport process thus resulting in a strong decrease of the oxygen-ion conductivity. However, when substitution increases to $x = 0.2$, the gallium–oxygen tetrahedra begin to appear in the iron–oxygen octahedral layers thus promoting oxygen vacancies in these layers and an increase of the ion conductivity to the level higher than in the ferrite with $x = 0.1$. Heating of the gallium-substituted samples results in the transition of the orthorhombic to CB structure similar to that in the undoped ferrite. It is argued that the high-temperature cubic structure is characterized by five-fold oxygen coordination of a small minority of the iron and gallium cations. The high-temperature cubic phase displays more thermodynamic stability than the low temperature orthorhombic phase. The introduction of gallium in the B cation sublattice is shown to generally disfavor electron–hole transport. However, electron and hole components of conductivity do not change in a regular manner with changes in gallium content and temperature. This peculiar behavior is explained as reflecting a complicated interplay of the disordering processes in the oxygen sublattice in response to gallium substitution and heating.

Acknowledgments

Authors are grateful to the Ural Branch of the Russian Academy of Science for support of this work under cooperation agreement #7-1. The present work has been also supported in part by the Grant #978002 from the NATO SfP program, and by the Chemical Sciences, Geosciences and Biosciences Division, Office of Basic Energy Sciences, Office of Science, US Department of Energy under Award #DE-FG02-03-ER15457.

References

- [1] Y. Teraoka, H.M. Zhang, S. Furukawa, N. Yamazoe, *Chem. Lett.* 7 (1988) 1084–1089.
- [2] Y. Takeda, K. Kanno, T. Takada, O. Yamamoto, M. Takano, N. Nakayama, Y. Bando, *J. Solid State Chem.* 63 (1986) 237–249.
- [3] J. Mizusaki, M. Okaysu, S. Yamauchi, K. Fueki, *J. Solid State Chem.* 99 (1992) 166–172.
- [4] P.K. Gallagher, J.B. MacChesney, D.N.E. Buchanan, *J. Chem. Phys.* 41 (1964) 2429–2434.
- [5] C. Greaves, A.J. Jacobson, B.C. Tofield, B.E.F. Fender, *Acta Crystallogr. B* 31 (1975) 641–646.
- [6] J.-C. Grenier, J. Darriet, M. Pouchard, P. Hagenmuller, *Mater. Res. Bull.* 11 (1976) 1219–1225.
- [7] M. Harder, H.K. Müller-Buschbaum, *Z. Anorg. Allg. Chem.* 464 (1980) 169–175.
- [8] S. Shin, M. Yonemura, H. Ikawa, *Mater. Res. Bull.* 13 (10) (1978) 1017–1021.
- [9] J.-C. Grenier, N. Ea, M. Pouchard, P. Hagenmuller, *J. Solid State Chem.* 58 (1985) 243–252.

- [10] M. Schmidt, S.J. Campbell, *J. Solid State Chem.* 156 (2001) 292–304.
- [11] V.L. Kozhevnikov, I.A. Leonidov, M.V. Patrakeeve, E.B. Mitberg, K.R. Poeppelmeier, *J. Solid State Chem.* 158 (2) (2001) 320–326.
- [12] M.V. Patrakeeve, E.B. Mitberg, A.A. Lakhtin, I.A. Leonidov, V.L. Kozhevnikov, V.V. Kharton, M. Avdeev, F.M.B. Marques, *J. Solid State Chem.* 167 (2) (2002) 203–213.
- [13] R.P. Shannon, *Acta Crystallogr. A* 32 (1976) 751–767.
- [14] L. Fournes, Y. Potin, J.C. Grenier, P. Hagemuller, *Rev. Phys. Appl.* 24 (2) (1989) 463–472.
- [15] M.V. Patrakeeve, J.A. Shilova, E.B. Mitberg, A.A. Lakhtin, I.A. Leonidov, V.L. Kozhevnikov, in: C. Julien, et al. (Eds.), *New Trends in Intercalation Compounds for Energy Storage*, vol. 61, Kluwer Academic Publishers, Dordrecht, The Netherlands, 2002, pp. 567–572.
- [16] P. Kofstad, *Nonstoichiometry, Diffusion and Electrical Conductivity in Binary Metal Oxides*, Wiley-Interscience, New York, 1972.
- [17] M.V. Patrakeeve, I.A. Leonidov, V.L. Kozhevnikov, V.V. Kharton, *Solid State Sci.* 6 (9) (2004) 907–913.